Study of oxygen reduction mechanism on Ag modified Sm1.8Ce0.2CuO4 cathode for solid oxide fuel cell

Li-Ping Sun, Qiang Li, Hui Zhao, Li-Hua Huo, Jean-Paul Viricelle, Christophe Pijolat

Study of oxygen reduction mechanism on Ag modified $Sm_{1.8}Ce_{0.2}CuO_4$ cathode for solid oxide fuel cell

Li-Ping Sun[1] — Hui Zhao[1] — Qiang Li[1] — Li-Hua Huo[1] — Jean-Paul Viricelle*[2] — Christophe Pijolat[2]

[1] Heilongjiang University, School of Chemistry and Materials Science, Key Laboratory of Functional Inorganic Material Chemistry

[2] Ecole Nationale Supérieure des Mines, SPIN-EMSE, PRESSIC, CNRS:UMR 5307, LGF, F-42023 Saint-Etienne, France

* Corresponding author: Tel: +33 4 77 42 02 52

E-mail address: viricelle@emse.fr

ABSTRACT

Different amount of metal silver particles are infiltrated into porous $Sm_{1.8}Ce_{0.2}CuO_4$ (SCC) scaffold to form SCC–Ag composite cathodes. The chemical stability, microstructure evolution and electrochemical performance of the composite cathode are investigated using X-ray diffraction (XRD), scanning electron microscopy (SEM), and AC impedance spectroscopy respectively. The composite cathode exhibits enhanced chemical stability. The metal Ag remains un-reacted with SCC and $Ce_{0.9}Gd_{0.1}O_{1.95}$ (CGO) at 800 °C for 72 h. The polarization resistance of the composite cathode decreases with the addition of metal Ag. The optimum cathode SCC-Ag05 exhibits the lowest area specific resistance (ASR, 0.43 Ω cm^2) at 700 °C in air. Investigation shows that metal Ag accelerates the charge transfer process in the composite cathode, and the rate limiting step for electrochemical oxygen reduction reaction (ORR) changes to oxygen dissociation and diffusion process.

KEYWORDS: Solid oxide fuel cell; Silver infiltration; Composite cathode; Electrode reaction

1 Introduction

One of the research targets for SOFCs is lowering the operating temperature in order to increase the life-time of the cell/stack/module as well as to reduce the cost of the materials. So far, many studies have been focused on the development of new electrode and electrolyte materials toward low temperature operable SOFCs [1], [2], [3] and [4]. Layered perovskite oxides with K_2NiF_4-type structure were extensively studied in recent years, due to their promising transport and catalytic properties, thermochemical stability and compatibility with other cell components [5], [6], [7], [8], [9], [10], [11], [12], [13], [14] and [15]. Among these oxides, Ln_2CuO_4 materials were found to exhibit excellent performance. For example, Li et al. reported that the ASR of the $La_{1.7}Sr_{0.3}CuO_4$ cathode was as low as 0.16 Ω cm^2 at 700 °C [16]. We studied the electrochemical performance of $Sm_{2-x}Ce_xCuO_4$ and the ASR of $Sm_{1.8}Ce_{0.2}CuO_4$ was found to be 1.16 Ω cm^2 at 700 °C [17]. Further research on the oxygen reduction kinetics of these cuprate cathodes always found that the charge transfer reaction was the rate limiting step [16], [17], [18], [19] and [20]. Thus, enhancing the oxygen reduction activity of these cathode materials is crucial for the development of novel IT-SOFC cathode.

Studies proved that cathodes infiltrated with Palladium (Pd) and platinum (Pt) metal particles showed promising oxygen reduction activity, due to the substantially increase of the surface catalysis properties [21] and [22]. Ag is another attractive infiltrating candidate than those precious metals, due to its good catalytic activity, high electrical conductivity and relatively low cost. Numerous works have been performed on the Ag-added perovskite cathodes [23], [24], [25], [26] and [27], but less attention was paid to the K_2NiF_4-type material [28].

To continue our studies on $Sm_{1.8}Ce_{0.2}CuO_4$ (referred as SCC in this paper) cathode materials, and to understand the effect of Ag doping on the electrode performance, SCC-Ag composite cathode was selected and the electrochemical property was studied compared with the bare SCC electrode. The mechanism of the oxygen reduction on the SCC-Ag composite cathode was investigated using electrochemical impedance spectroscopy (EIS) technique.

2 Experimental

$Sm_{1.8}Ce_{0.2}CuO_4$ powder was synthesized using the glycine-nitrate process (GNP). According to the formula, stoichiometric amount of metal nitrates were mixed in a beaker to form a solution, and then glycine (aminoacetic acid, $H_2NCH_2CO_2H$) was added into the nitrate solution at 1:2 M ratio of metal ions/glycine according to propellant chemistry. After drying and firing, the resultant powder was calcined in air at 1000 °C for 12 h. The $Ce_{0.9}Gd_{0.1}O_{1.95}$ (CGO) powder (Rhodia Courbevoie, France) was pressed uniaxially at 220 MPa and sintered at 1400 °C for 10 h to form a densified pellet. In order to perform EIS measurement, a test cell with three electrodes configuration was constructed. The $Sm_{1.8}Ce_{0.2}CuO_4$ powder was mixed with terpineol to form a slurry, and subsequently painted on one side of the CGO electrolyte pellet to form an electrode area of 0.5 cm^2, used as working electrode (WE). The WE was first heated at 400 °C for 2 h to eliminate organic binders, followed by sintering at 1000 °C for 4 h in air, with a heating/cooling rate of 3 °C min^{-1}. Platinum paste was painted on the other side of the CGO pellet in symmetric configuration, and then sintered at 800 °C for 1 h in air, to form porous counter electrode (CE). A Pt wire was used as reference electrode (RE) and put on the same side of the working electrode. Silver nitrate solution was then infiltrated into the porous cathode. The detail of infiltration process was as follows: 0.05 mol L^{-1} $AgNO_3$ solution was prepared by dissolving silver nitrate powders in mixture solution of distilled water and ethanol. Ethanol was added to reduce the surface tension on SCC

backbone. The ratio of ethanol to water is 1 to 1. The infiltration was carried out in a vacuum chamber by dripping the $AgNO_3$ solution onto the SCC cathode area carefully using an injector and drying at 80 °C. The infiltrated cathode was then calcined at 800 °C for one hour. This infiltration step was repeated several times to obtain a suitable weight of Ag loaded on the SCC backbone. The obtained cathodes with different weight ratio of Ag were abbreviated as SCC-Ag02 for $Sm_{1.8}Ce_{0.2}CuO_4$ with 2 wt.% Ag, SCC-Ag05 for $Sm_{1.8}Ce_{0.2}CuO_4$ with 5 wt.% Ag, and so on.

In order to check the chemical stability of SCC with CGO at high temperature, these two components were mixed thoroughly in 1:1 weight ratio, and heat-treated at 1000 °C for 4 h in air. Silver nitrate was then added to the mixture, and again heated up to 800 °C for 72 h to form SCC–CGO–Ag composite powders.

The sample was characterized using X-ray diffraction instrument (Rigaku, D/MAX-3B) and scanning electron microscopy (SEM) (Hitachi, S-4700 FEG), respectively. The impedance spectra were recorded over the frequency range 1 MHz to 0.1 Hz using Autolab PGStat30. The measurements were performed at OCV as a function of temperature (550–700 °C) and oxygen partial pressure (in N_2/O_2 mixed atmosphere).

3 Results and discussion

Phase purity of the prepared SCC and chemical compatibility of Ag metal with SCC and CGO were first investigated. Fig. 1 shows XRD patterns of the sintered SCC–CGO and SCC–CGO–Ag composite powders. The spectra of pure SCC and CGO materials are also presented in the same figure for comparison. The SCC powder made by GNP process crystallizes in body-centered tetragonal symmetry (Fig. 1(a)), consisting with Sm_2CuO_4 structure (PDF card

No. 24-0998). After sintered at 1000 °C for 4 h, SCC and CGO retained their own structures in the SCC–CGO mixture (Fig. 1(c)). When Ag was added and the composite cathode was then heated at 800 °C for prolonged 72 h, no additional peaks except those from metal Ag, SCC and CGO can be detected (Fig. 1(d)). This result indicates that Ag is highly chemical compatible with SCC and CGO materials.

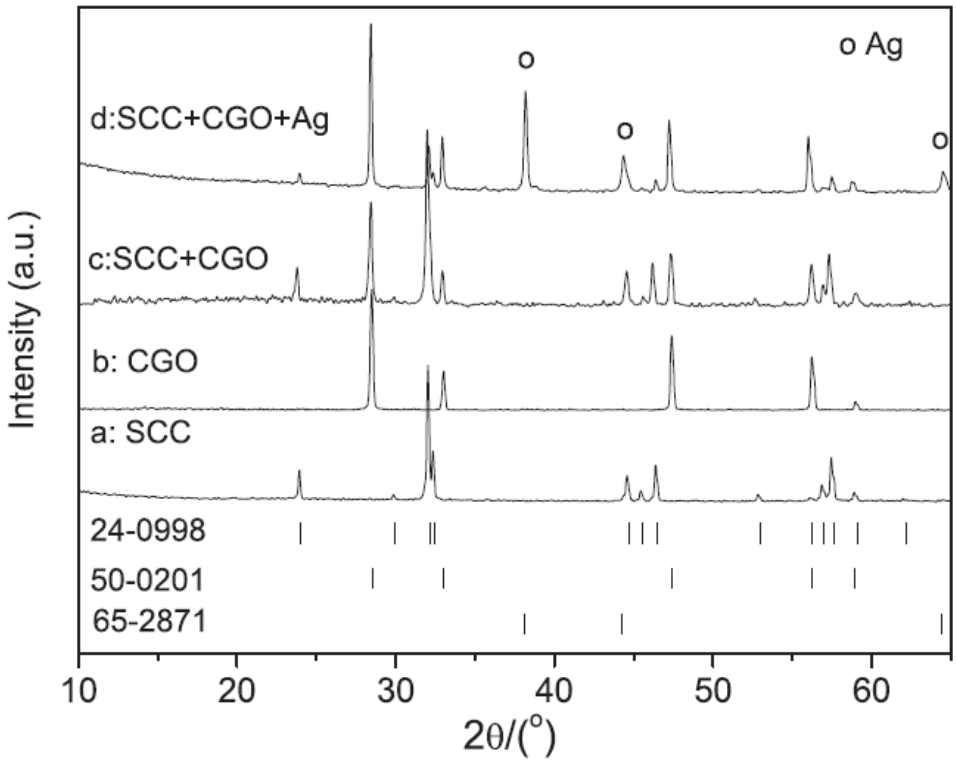

Fig. 1: XRD patterns of SCC, CGO, SCC–CGO and SCC–CGO–Ag powders.

The SEM images of SCC and SCC–Ag cathodes are comparably shown in Fig. 2. Obviously a fine microstructure with moderate porosity and well-necked particles is formed in the SCC cathode after firing at 1000 °C for 4 h (Fig. 2(A)). The impregnation of Ag does not change the microstructure adversely. Some round-shape particles are found in the SCC-Ag05 cathode after the infiltration of $AgNO_3$ and then firing at 800 °C for 1 h (Fig. 2(B)). The surface mapping result indicates that these round-shape particles are metallic Ag, which are dispersed uniformly on the surface of the cathode (Fig. 2(C)). The average particle size of Ag is about 1–2 μm. The cross-sectional image of the SCC-Ag05 cathode and the CGO electrolyte is

presented in Fig. 2(D). Clearly the cathode and the electrolyte form good contact with each other. These is no delamination or cracking that be observed at the electrode/electrolyte interface. The thickness of the electrode is about 15 μm (Fig. 2(D)). The EDX result further supports that metal Ag is distributed in the SCC-Ag05 cathode (Fig. 2(D), inset). When the Ag loading increases to 10 wt.%, however, the glomeration and growth of Ag particles can be visualized (Fig. 2(E)). This aggregation results in less TPBs and thus be suspected to increase the polarization resistance.

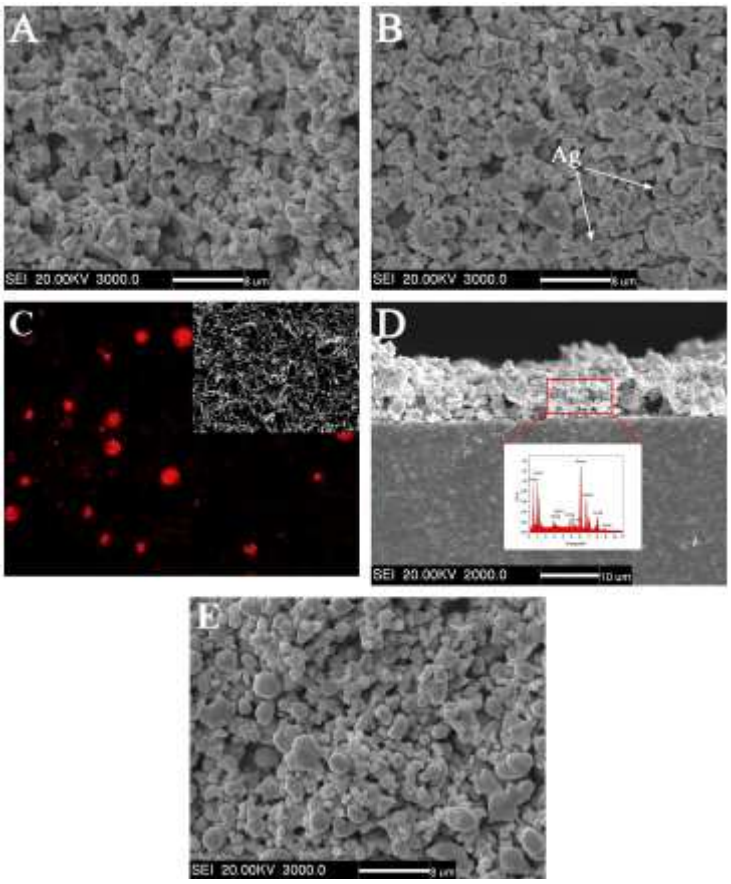

Fig. 2: SEM micrographs of the cathodes: (A) SCC without Ag (1000 °C, surface), (B) SCC-Ag05 (800 °C, surface), (C) EDS elemental Mapping to show the spatial distribution of metallic Ag (red), inset shows the mapping area of SCC-Ag05 cathode: (D) SCC-Ag05 (800 °C, cross-sectional image), inset is the EDX result of the cross-sectional part of SCC-Ag05 cathode, (E) SCC with 10 wt.% Ag (800 °C, surface).

To explore the effects of Ag loading on polarization resistance, the impedance spectra of SCC cathode impregnated with different amounts of Ag were measured (Fig. 3). For all the cathodes, the impedance spectra can be separated into two arcs located in the high-frequency zone and the low-frequency zone respectively, implying two consecutive reaction processes related to oxygen reduction reaction (ORR) might take place. The overall size of the two arcs is primarily attributed to the cathode area specific resistance (ASR), which is widely used to describe the resistance terms related to electrode process. The Arrhenius plots of ASR are given in Fig. 4. Obviously the activation energy (*Ea*) of SCC–Ag cathode is much smaller than SCC cathode. The ASR decreases with the Ag content, reaches a minimum at 5 wt.% Ag, and then increases again at 10 wt.% Ag. The variation of ASR with Ag contents can be understood, considering that the ORR process of the SCC electrode is likely promoted by the surface modification with silver. However, with the further increase of Ag content in the composite cathode, some surface of the SCC particles may be covered by the Ag metal, and the active sites for oxygen reduction reaction will be reduced. This deduction was proved by fitting the impedance spectra with an equivalent circuit (Fig. 3, inset) composed of two R-CPE elements in series to obtain the resistance of different processes. In this equivalent circuit, R_{ohm} represents the combination of electrolyte resistance, electrode ohmic resistance, lead resistance and contact resistance between cathode and Pt mesh current collector, R_H and R_L are the polarization resistance (R_p) corresponding to the high-frequency and low-frequency arc, respectively. The ASR is the sum of R_H and R_L. CPE is constant phase element whose value reflects the reaction mechanism of different electrode processes. The fitting results are presented in Fig. 5. It can be seen that R_H is much larger than R_L in SCC cathode. In a previous study, we proved that the reaction rate limiting step of SCC cathode was charge transfer reaction, which was characterized by the high frequency arc in the EIS spectrum [17]. Compared to SCC electrode, the addition of Ag reduces dramatically the value of ASR and

the decrease is mainly attributed by the reduction of R_H. Arrhenius plots of the fitting results for SCC–Ag composite cathode are given in Fig. 6. It is found that both R_H and R_L first decreases with the addition of Ag, and then increases again when the Ag content is up to 10 wt.% in the SCC–Ag composite. The activation energy for R_H is in the range of 1.52–1.55 eV, close to the activation energy of the oxygen surface exchange process in $La_2NiO_{4+\delta}$ [5]. At the same time, the low frequency arc becomes dominant in the impedance spectra (Fig. 3), and the values of R_L are larger than these of R_H in the SCC–Ag composite cathodes (Fig. 6). The activation energy for R_L is in the range of 0.96–1.16 eV, which is close to the dissociation and diffusion activation energy of the adsorbed oxygen molecular on the cathode surface [29]. The contribution of Ag loading is further illustrated in the Bold plot (Fig. 7). The enhanced charge transfer reaction can be seen by a dramatic decrease of the phase angle of the high frequency peak in the Bold plot. This is clearly different from that of SCC cathode. According to the fitting results, this difference indicates that the oxygen reduction mechanism has been changed with the addition of Ag.

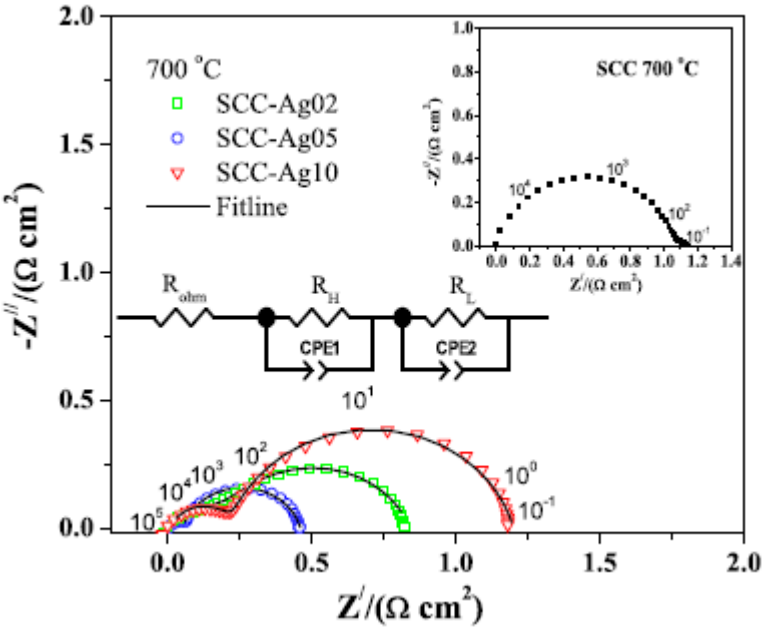

Fig. 3: Nyquist plot for SCC–Ag composite cathodes measured at 700 °C in air.

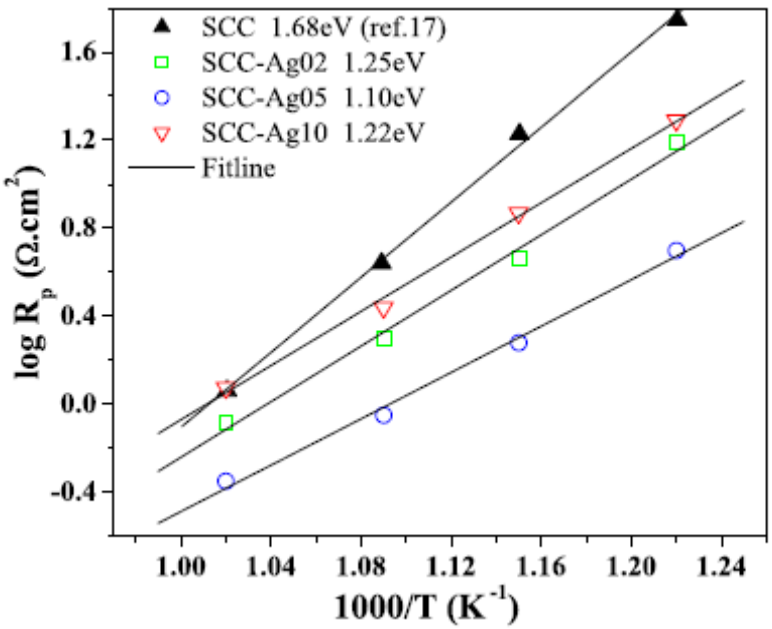

Fig. 4: Temperature dependence of the polarization resistance R_p for various SCC-xAg composites measured in air.

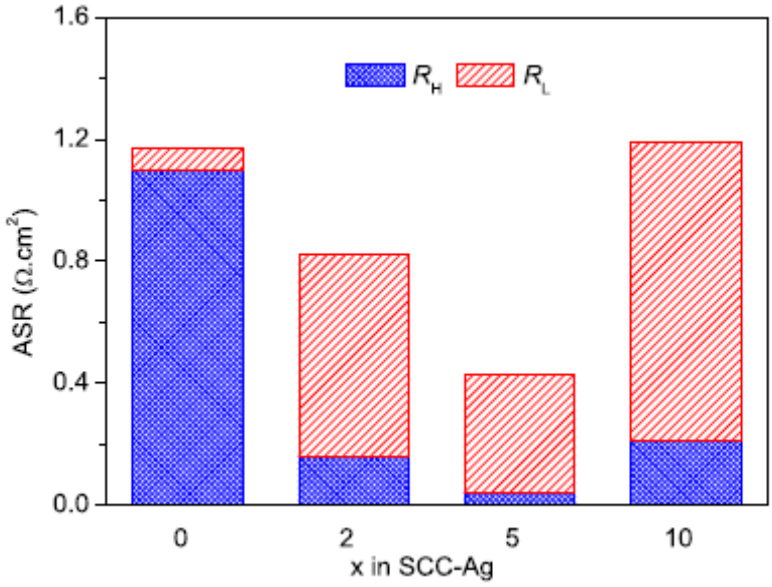

Fig. 5: Comparative evolution of the polarization resistance (R_H and R_L) with different amount of Ag in the SCC–Ag composite cathode.

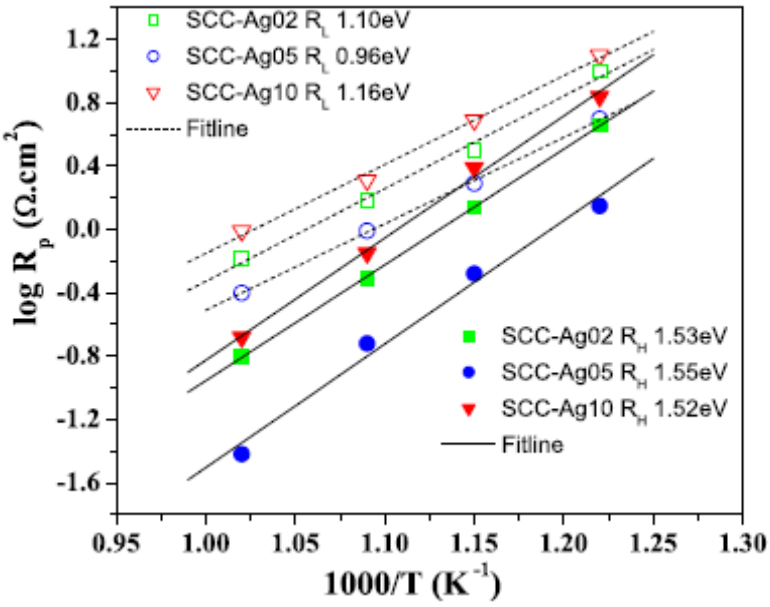

176

177 Fig. 6: Temperature dependences of fitted high frequency resistances and low frequency

178 resistances of the SCC–Ag composite electrodes with different Ag content.

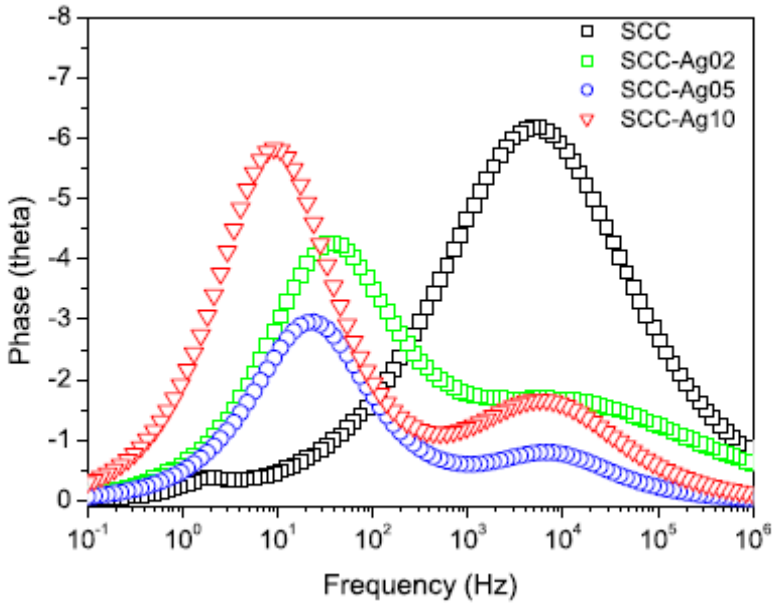

179

180 Fig. 7: Bold plot for SCC–Ag composite cathodes measured at 700 °C in air.

181 The electrochemical reaction mechanism of SCC–Ag composite cathode was studied as a

182 function of oxygen partial pressure. Fig. 8 shows the impedance spectra of SCC-Ag05

183 cathode measured at 700 °C under various oxygen partial pressures (P_{O_2}). The polarization

184 resistance decreases with the increase of oxygen partial pressure, indicating an oxygen

activity related electrochemical reaction that occurred on the composite cathode. By using the same equivalent circuit presented in Fig. 3, the values of R_H and R_L under different oxygen partial pressure can be calculated. It is found that the resistance of the high frequency arc (R_H) is always much smaller than that of the low frequency one (R_L). This means that the R_L related process is the reaction rate limiting step. Generally, the polarization resistance (R_p) varies with the oxygen partial pressure according to the following equation:

$$R_P = R_P^0 \; x \; (P_{O_2})^n$$

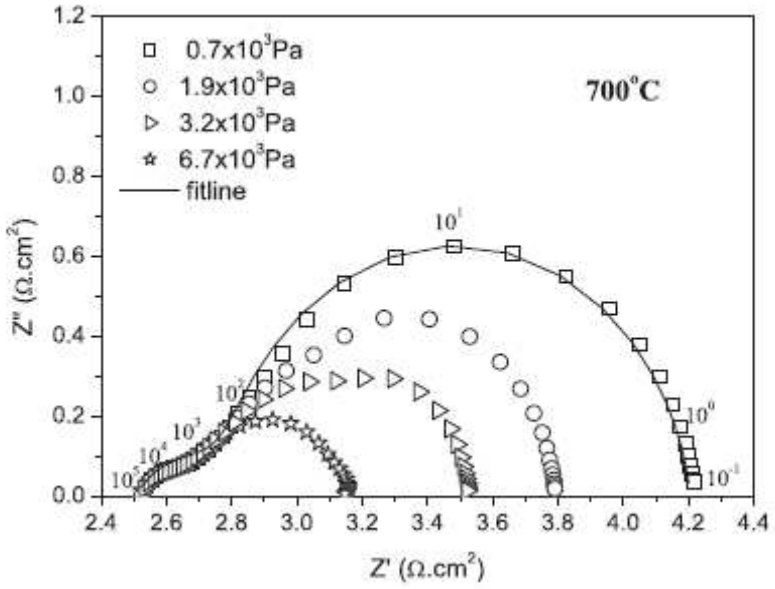

Fig. 8: Impedance spectra for the SCC-Ag05 cathode on CGO at 700 °C under various oxygen partial pressures.

The value of *n* could give useful information about the type of species involved in the reactions [30] and [31]:

$n = 1 \quad O_2(g) \Leftrightarrow O_{2ads.}$

$n = 0.5 \quad O_{2ads.} \Leftrightarrow 2O_{ads.}$

$n = 0.25 \quad O_{ads.} + 2e^{'} + V_O^{\bullet\bullet} \Leftrightarrow O_O^x$

$n = 0 \quad O_{TPB}^{2-} + V_O^{\bullet\bullet} \Leftrightarrow O_O^x$

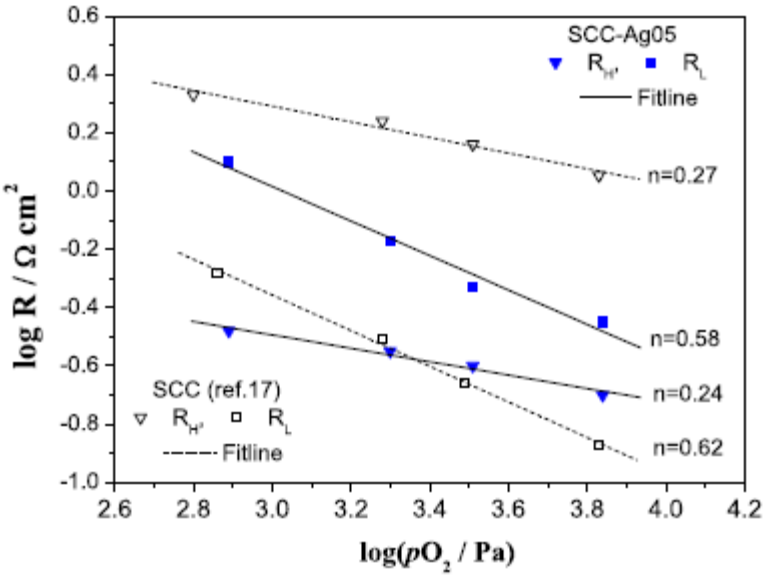

Fig. 9: Dependence of polarization resistance on oxygen partial pressure for SCC-Ag05 composite cathode at 700 °C.

The dependence of polarization resistances (R_H and R_L, respectively) on oxygen partial was presented in Fig. 9. It is found that the values of n corresponding to R_H and R_L are 0.24 and 0.58 respectively. In this case the high frequency arc is confirmed to be related to the charge transfer process, and the low frequency arc is assigned to the dissociation and diffusion of adsorbed oxygen. Compared to the results obtained in Fig. 8, it is clear that the R_L related process is the major rate limiting step for SCC-Ag05 composite cathode in the whole range of measurement oxygen partial pressure. However for SCC cathode, the n values of R_H and R_L are 0.27 and 0.62 respectively, and the value of R_H is always larger than R_L, which implied that the charge transfer process on SCC cathode is the rate limiting step [17]. So it is clear that when Ag was added in the electrode, a change of the rate limiting step from charge transfer process to diffusion of the dissociative adsorbed oxygen was likely happened. As we expected, Ag catalyst promotes the surface exchange process (charge transfer reaction) and additionally, Ag particles can provide additional electron transport pathway through the cathode surface due to its high electronic conductivity. Therefore, the oxygen reduction reaction could be more effective at the boundary of Air/Ag/SCC than at Air/SCC, and

consequently the electrochemical performance is enhanced by the impregnation of Ag catalyst.

It should point out that the great reduce of R_H value is paid back by the simultaneous increase of R_L (Fig. 5). It is proposed that this simple infiltration method used may lead to the growth of micrometer size Ag particles, which will cover the SCC particle surface and block the oxygen diffusion channel in the cathode. So the microstructure of the cathode need to be further optimized.

4 Conclusion

The $Sm_{1.8}Ce_{0.2}CuO_4$–Ag composite cathodes were prepared and their electrochemical properties were studied below 700 °C. The SCC-Ag05 composite exhibits improved catalytic activity for the oxygen reduction reaction compared to the $Sm_{1.8}Ce_{0.2}CuO_4$ cathode, due to the increased electronic conductivity and electro-catalytic activity contributed by Ag particles. The lowest area specific resistance obtained at 700 °C in air is 0.43 Ω cm^2 for SCC-Ag05 composite cathode. The addition of Ag in the SCC electrode changes the rate limiting step from charge transfer process to oxygen dissociation and diffusion process. However, further long-term stability investigation by operating over an extended period may be needed to verify the effect of Ag diffusion.

Acknowledgments

This work was supported by National Natural Science Foundation of China (51072048, 51102083), Natural Science Foundation of Heilongjiang Province (JC201211, B201107), Program for Science and Technology Project of Heilongjiang Province (WB10A204).

References

[1] D. Brett, A. Atkinson, N.P. Brandon, S.J. Skinner, Intermediate temperature solid oxide fuel cells, Chem Soc Rev, 37 (2008), pp. 1568–1578

[2] B.C.H. Steele, A. Heinzel, Materials for fuel-cell technologies, Nature, 414 (2001), pp. 345–352

[3] C. Xia, Y. Li, Y. Tian, Q. Liu, Y. Zhao, L. Jia et *al.*, A high performance composite ionic conducting electrolyte for intermediate temperature fuel cell and evidence for ternary ionic conduction, J Power Sources, 188 (2009), pp. 156–162

[4] W. Zhou, Z.P. Shao, Z.G. Liang, Z.H. Zhu, W.Q. Jin, N.P. Xu, A new cathode for solid oxide fuel cells capable of in situ electrochemical regeneration, J Mater Chem, 21 (2011), pp.

[5] S.J. Skinner, J.A. Kilner, Oxygen diffusion and surface exchange in $La_{2-x}Sr_xNiO_{4+\delta}$, Solid State Ionics, 135 (2000), pp. 709–712

[6] V.V. Kharton, A. Viskup, E. Naumovich, F. Marques, Oxygen ion transport in La_2NiO_4-based ceramics, J Mater Chem, 9 (1999), pp. 2623–2629

[7] A. Hernández, L. Mogni, A. Caneiro, $La_{2-x}Sr_xNiO_{4+\delta}$ as cathode for SOFC: reactivity study with YSZ and CGO electrolytes, Int J Hydrogen Energy, 35 (2010), pp. 6031–6036

[8] J. Huang, R. Gao, Z. Mao, J. Feng, Investigation of $La_{2-x}Sr_xNiO_{4+\delta}$ based cathodes for SDC -carbonate composite electrolyte intermediate temperature fuel cells, Int J Hydrogen Energy, 35 (2010), pp. 2657–2662

[9] M.A. Daroukh, V.V. Vashook, H. Ullmann, F. Tietzb, I.A. Raj, Oxides of the AMO_3 and A_2MO_4- type: structural stability, electrical conductivity and thermal expansion, Solid State Ionics, 158 (2003), pp. 141–150

[10] Y.S. Wang, H.W. Nie, S.R. Wang, T.L. Wen, U. Guth, V. Valshook, $A_{2-\alpha}A_{\alpha'}BO_4$-type oxides as cathode materials for IT-SOFCs(A = Pr, Sm; A′ = Sr; B = Fe, Co), Mater Lett, 60 (2006), pp. 1174–1178

[11] H. Zhao, F. Mauvy, C. Lalanne, J.M. Bassat, S. Fourcade, J.C. Grenier, New cathode materials for ITSOFC: phase stability oxygen exchange and cathode properties of $La_{2-x}NiO_{4+\delta}$, Solid State Ionics, 179 (2008), pp. 2000–2005

[12] F. Mauvy, C. Lalanne, J.M. Bassat, J.C. Grenier, H. Zhao, P. Dordor *et al.*, Oxygen reduction on porous $Ln_2NiO_{4+\delta}$ electrodes, J Eur Ceram Soc, 25 (2005), pp. 2669–2672

[13] L.P. Sun, Q. Li, L.H. Huo, H. Zhao, G.Y. Zhang, N. Lin *et al.*, Synthesis and performance of $Sr_{1.5}La_xMnO_4$ as cathode materials for intermediate temperature solid oxide fuel cell, J Power Sources, 196 (2011), pp. 5835–5839

[14] J. Dailly, S. Fourcade, A. Largeteau, F. Mauvy, J. Grenier, M. Marrony, Perovskite and A_2MO_4 -type oxides as new cathode materials for protonic solid oxide fuel cells, Electrochim Acta, 55 (2010), pp. 5847–5853

[15] G. Taillades, J. Dailly, M. Taillades-Jacquin, F. Mauvy, A. Essouhmi, M. Marrony *et al.*, Intermediate temperature anode-supported fuel cell based on $BaCe_{0.9}Y_{0.1}O_3$ electrolyte with novel Pr_2NiO_4 cathode, Fuel Cells, 10 (2010), pp. 166–173

[16] Q. Li, H. Zhao, L.H. Huo, L.P. Sun, X.L. Cheng, J.C. Grenier, Electrode properties of Sr doped La_2CuO_4 as new cathode material for intermediate-temperature SOFCs, Electrochem Commun, 9 (2007), pp. 1508–1512

[17] L.P. Sun, L.H. Huo, H. Zhao, Synthesis and performance of $Sm_{2-x}Ce_xCuO_4$ cathode materials for IT-SOFC, Chin J Inorg Chem, 23 (2007), pp. 1545–1549

[18] Q. Li, X. Zeng, L.P. Sun, H. Zhao, L.H. Huo, J.C. Grenier, Electrochemical performance of $La_2Cu_{1-x}Co_xO_4$ cathode materials for intermediate- temperature SOFCs, Int J Hydrogen Energy, 37 (2012), pp. 2552–2558

[19] J.H. Hao, Q. Li, L.P. Sun, H. Zhao, L.H. Huo, Synthesis and performance of $Nd_{2-x}Sr_xCuO_4$ cathode materials for IT-SOFC, Chin J Inorg Chem, 25 (2009), pp. 1818–1822

[20] L.P. Sun, H. Zhao, Q. Li, L.H. Huo, J.P. Viricelle, C. Pijolat, Study on $Sm_{1.8}$Ce0.2CuO4-$Ce_{0.9}Gd_{0.1}O_{1.95}$ composite cathode materials for intermediate temperature solid oxide fuel cell, Int J Hydrogen Energy, 36 (2011), pp. 12555–12560

[21] H.J. Hwang, J.W. Moon, S. Lee, E.A. Lee, Electrochemical performance of LSCF-based composite cathodes for intermediate temperature SOFCs, J Power Sources, 145 (2005), pp. 243–248

[22] T.J. Huang, X.D. Shen, C.L. Chou, Characterization of Cu, Ag and Pt added $La_{0.6}Sr_{0.2}Co_{0.2}Fe_{0.8}O_{3-\delta}$ and gadolinia-doped ceria as solid oxide fuel cell electrodes by temperature-programmed techniques, J Power Sources, 187 (2009), pp. 348–355

[23] Y. Lin, R. Ran, Z. Shao, Silver-modified $Ba_{0.5}Sr_{0.5}Co_{0.8}Fe_{0.2}O_{3-\delta}$ as cathodes for a proton conducting solid-oxide fuel cell, Int J Hydrogen Energy, 35 (2010), pp. 8281–8288

[24] Y. Sakito, A. Hirano, N. Imanishi, Y. Takeda, O. Yamamoto, Y. Liu, Silver infiltrated cathodes for intermediate temperature solid oxide fuel cells, J Power Sources, 182 (2008), pp. 476–481

[25] I. Wilkinson, J. Zhu, Ag-perovskite composite materials for SOFC cathode-interconnect contact, J Electrochem Soc, 156 (2009), pp. B905–B912

[26] T. Suzuki, Y. Takahashi, K. Hanamoto, T. Yamaguchi, Y. Fujishiro, Low temperature processed composite cathodes for solid-oxide fuel cells, Int J Hydrogen Energy, 36 (2011), pp. 10998–11003

[27] T.J. Huang, C.L. Chou, Oxygen dissociation and interfacial transfer rate on performance of SOFCs with metal-added (LaSr)(CoFe)O_3-(Ce, Gd)$O_{2-\delta}$ cathodes, Fuel Cells, 10 (2010), pp. 718–725

[28] Q. Li, L.P. Sun, L.H. Huo, H. Zhao, J. Grenier, Electrochemical performance of $La_{1.6}Sr_{0.4}NiO_4$- Ag composite cathodes for intermediate-temperature solid oxide fuel cells, J Power Sources, 196 (2011), pp. 1712–1716

[29] Y.P. Yin, B.W. Liu, J.J. Qi, Y.S. Gu, Q.L. Liao, Z. Qin *et al.*, Characterization of $Ba_{1.0}Sr_{1.0}FeO_{4+\delta}$ cathode on $La_{0.9}Sr_{0.1}Ga_{0.8}Mg_{0.2}O_{3-\delta}$ electrolyte for intermediate temperature solid oxide fuel cells, J Power Sources, 196 (2011), pp. 6238–6241

[30] G. Zhan, X.M. Liu, B. Bergman, Z. Zhao, Investigation of oxygen reduction reaction kinetics on $Sm_{0.5}Sr_{0.5}CoO_{3-\delta}$ cathode supported on Ce0.85Sm0.075Nd0.075O2−δ electrolyte, J Power Sources, 196 (2011), pp. 9195–9203

[31] J.D. Kim, G.D. Kim, J.W. Moon, Y. Park, W.H. Lee, K. Kobayashi *et al.*, Characterization of LSM-YSZ composite electrode by ac impedance spectroscopy, Solid State Ionics, 143 (2001), pp. 379–389